

## Effects of Cyclodextrins on the Fluorescence of 2-Methylnaphth[2,3-*d*]oxazole in Aqueous Solution

Sanyo Hamai

Department of Chemistry, Faculty of Education and Human Studies, Akita University,  
Tegata Gakuen-machi 1-1, Akita 010-8502

Received March 22, 2004; E-mail: hamai@ipc.akita-u.ac.jp

In organic solvents, 2-methylnaphth[2,3-*d*]oxazole (MNO) exhibits a single emission, whereas it exhibits dual emissions (the 350-nm band fluorescence and the longer-wavelength fluorescence) in water (pH 6.1). In acidic aqueous solution, the 350-nm band fluorescence alone is observed with a disappearance of the longer-wavelength fluorescence. In pH 6.1 buffers,  $\alpha$ -CD has been found to form a 2:1 inclusion complex with MNO. Upon the addition of  $\alpha$ -CD to MNO solution, the longer-wavelength fluorescence is significantly reduced in intensity, relative to the 350-nm band fluorescence. The incorporation of an MNO molecule into the  $\alpha$ -CD cavities obstructs the generation of the excited state responsible for the longer-wavelength fluorescence. The longer-wavelength fluorescence is most likely due to the intramolecular charge transfer (ICT) state of MNO, which is induced by water molecules of high polarity. MNO forms a 1:1 inclusion complex with  $\beta$ -CD. In the presence of  $\beta$ -CD, the intensity ratio of the longer-wavelength fluorescence to the 350-nm band fluorescence is decreased. When 1-propanol is added to MNO solution containing  $\beta$ -CD, a ternary inclusion complex is formed among  $\beta$ -CD, MNO, and 1-propanol. In  $\beta$ -CD solution containing 1-propanol, the intensity ratio of the longer-wavelength fluorescence to the 350-nm band fluorescence is slightly reduced. These findings support the conclusion that the longer-wavelength fluorescence of MNO is due to the ICT state, whose generation is promoted by the water environment.

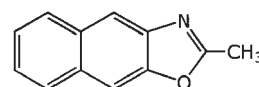
Cyclic oligosaccharides composed of six, seven, and eight D-glucopyranose residues are called  $\alpha$ -cyclodextrin ( $\alpha$ -CD),  $\beta$ -cyclodextrin ( $\beta$ -CD), and  $\gamma$ -cyclodextrin ( $\gamma$ -CD), respectively; they are shaped like a truncated cone with a hollow cavity. CDs, which have many hydroxy groups on their narrow and wide rims, are soluble in water. Because the inner wall of the CD cavity is relatively hydrophobic, CD forms inclusion complexes with a variety of organic compounds in aqueous solution.<sup>1,2</sup> In inclusion complexes, the physico-chemical properties of guest molecules are affected. This enables us to use CDs not only in some application fields but also in some research fields. From a photochemical point of view, the photo-Fries rearrangement of phenyl esters has been studied in the presence of CD.<sup>3–5</sup> For meta-substituted phenyl-ester and anilides in aqueous solutions containing ten-fold excess of  $\beta$ -CD, a remarkable ortho selectivity has been observed.<sup>6,7</sup>

Dual emissions of *p*-dimethylaminobenzonitrile (DMABN) have been investigated in aqueous solutions containing CDs.<sup>8–10</sup> In a complex in which a DMABN molecule is totally enclosed inside the  $\gamma$ -CD cavity, the formation of the twisted intramolecular charge transfer (TICT) state is significantly suppressed, accompanied by a large enhancement of the locally excited state emission, whereas in a partially enclosed DMABN molecule the TICT emission is only slightly enhanced.<sup>10</sup> As shown in the case of DMABN, the emission and molecular properties of a fluorophore can be examined using CDs.

2-(4-Aminophenyl)- and 2-[4-(*N,N*-dimethylamino)phenyl]-benzothiazole (APB and DAPB) exhibit a single fluorescence band in aqueous solution.<sup>11</sup> The encapsulation of these benzothiazole derivatives by  $\beta$ -CD has been studied in aqueous solu-

tion. The binding constants of APB and DAPB for  $\beta$ -CD have been evaluated to be  $1542 \pm 50$  and  $5664 \pm 50 \text{ mol}^{-1} \text{ dm}^3$ , respectively.<sup>11</sup> Several oxazole derivatives, which are analogous in structure to a thiazole compound, are frequently used as scintillators. For 2-(2'-hydroxyphenyl)oxazole, dual fluorescence has been observed in polar and protic solvents due to several ground-state tautomers.<sup>12</sup>

However, the photophysical properties of oxazole derivatives have seldom been studied in water. 2-Methylnaphth[2,3-*d*]oxazole (MNO) is an oxazole derivative, in which an oxazole ring is fused to a naphthalene ring (Scheme 1). We have found that in aqueous solution (pH 6.1), MNO exhibits the longer-wavelength fluorescence besides the 350-nm band fluorescence that appears in organic solvents and water. MNO, which has a naphthalene ring, is expected to be bound to the CD cavity, because CD includes a naphthalene moiety. Consequently, the origin of the longer-wavelength fluorescence of MNO can be investigated using CDs as perturbers for the environment around an MNO molecule in water. Through the interactions of CDs with MNO, we have examined the emission properties including the longer-wavelength fluorescence.



2-Methylnaphth[2,3-*d*]oxazole  
(MNO)

Scheme 1.

## Experimental

MNO, which was purchased from Tokyo Kasei Kogyo, was twice recrystallized from ethanol.  $\beta$ -CD, obtained from Nacalai Tesque, was twice recrystallized from water, while  $\alpha$ -CD and  $\gamma$ -CD, which were obtained from Nacalai Tesque and Wako Pure Chemical Industries, respectively, were used without further purification. Buffers ( $5.3 \times 10^{-3}$  mol dm $^{-3}$  of KH $_2$ PO $_4$  and  $1.3 \times 10^{-3}$  mol dm $^{-3}$  of Na $_2$ HPO $_4$ ) of pH 6.1 were used throughout this work. MNO aqueous solution used for the preparation of sample solutions was prepared by allowing purified MNO crystals to plunge into water for a few days. The concentrations of MNO in aqueous solutions have been calculated under the assumption that, at an absorption peak, the molar absorption coefficient of MNO in water is the same as that in ethanol.

Absorption spectra were recorded on a Shimadzu UV-260 spectrophotometer. Fluorescence spectra were taken with a Shimadzu RF-501 spectrofluorometer equipped with a cooled Hamamatsu R-943 photomultiplier. The fluorescence spectra were corrected for the spectral response of the fluorometer. Spectroscopic measurements were made at  $25 \pm 0.1$  °C.

## Results and Discussion

**Absorption and Fluorescence Spectra of MNO in Organic Solvents and Water.** Figure 1 shows absorption spectra of MNO ( $5.0 \times 10^{-5}$  mol dm $^{-3}$  except for water ( $5.1 \times 10^{-5}$  mol dm $^{-3}$ )) in cyclohexane, ethanol, acetonitrile, and water. In the polar solvents, the absorption bands of MNO are blurred compared to those in cyclohexane. The absorption peaks of MNO are very slightly blue-shifted on going from cyclohexane to water.

Figure 2 exhibits fluorescence spectra of MNO ( $5.0 \times 10^{-5}$  mol dm $^{-3}$  except for water ( $5.1 \times 10^{-5}$  mol dm $^{-3}$ )) in cyclohexane, ethanol, acetonitrile, and water. The fluorescence intensity in water is reduced with a blurring of the fluorescence band, compared to that in cyclohexane. In addition to the 350-nm band fluorescence, which is assigned to the locally excited-state (LE) emission, MNO in water exhibits a broad, longer-wavelength emission. In Fig. 2, the longer-wavelength emission is apparently maximized at around 400 nm. The fluores-

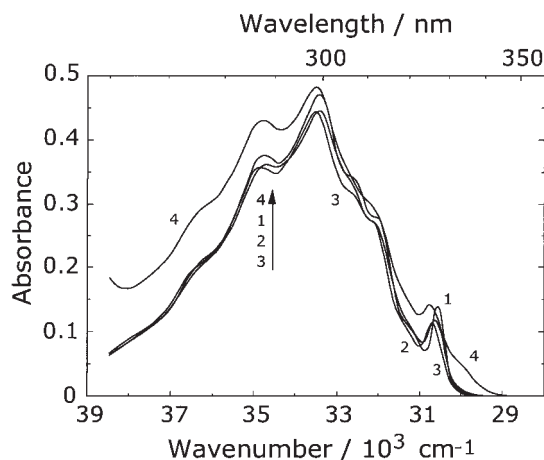


Fig. 1. Absorption spectra of MNO ( $5.0 \times 10^{-5}$  mol dm $^{-3}$  except for water ( $5.1 \times 10^{-5}$  mol dm $^{-3}$ )) in cyclohexane (spectrum 1), ethanol (spectrum 2), acetonitrile (spectrum 3), and water (spectrum 4).

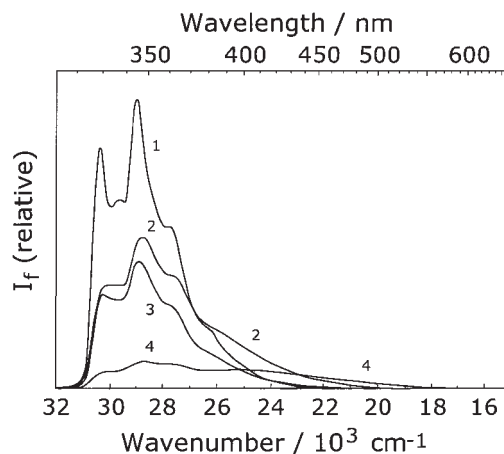


Fig. 2. Fluorescence spectra of MNO ( $5.0 \times 10^{-5}$  mol dm $^{-3}$  except for water ( $5.1 \times 10^{-5}$  mol dm $^{-3}$ )) in cyclohexane (spectrum 1), ethanol (spectrum 2), acetonitrile (spectrum 3), and water (spectrum 4).  $\lambda_{\text{ex}} = 304$  nm.

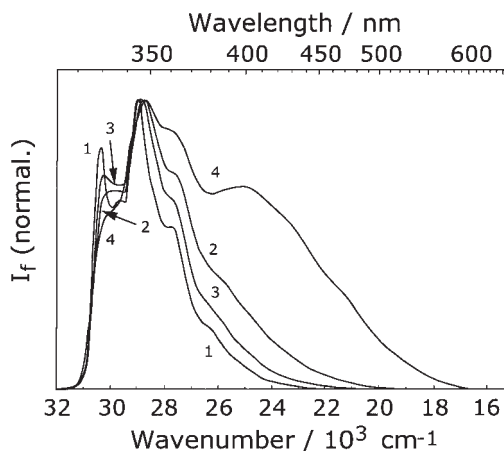


Fig. 3. Normalized fluorescence spectra of MNO ( $5.0 \times 10^{-5}$  mol dm $^{-3}$  except for water ( $5.1 \times 10^{-5}$  mol dm $^{-3}$ )) in cyclohexane (spectrum 1), ethanol (spectrum 2), acetonitrile (spectrum 3), and water (spectrum 4).  $\lambda_{\text{ex}} = 304$  nm.

cence excitation spectra of MNO observed at 350 and 450 nm are the same, indicating that the longer-wavelength emission is not due to an impurity (impurities). The normalized fluorescence spectra of MNO in the organic solvents and water are depicted in Fig. 3. The fluorescence peak is very slightly red-shifted on going from cyclohexane to the polar solvents. The difference in equilibrium bond length of the potential energy curve between the ground and excited states may be varied by the solvent polarity. This probably explains the blue shift in the absorption peak and the red shift in the fluorescence peak in the polar solvents.

From a titration curve that shows the absorbance of MNO at 288 nm, a  $pK_a$  value of MNO has been evaluated to be 3.23. This finding indicates that MNO exists as a neutral species at pH 6.1. Figure 4 illustrates fluorescence spectra of MNO ( $5.1 \times 10^{-5}$  mol dm $^{-3}$ ) in aqueous solutions at various pH values. In acidic solutions, where the protonation to the nitrogen atom in MNO most likely occurs, MNO shows only the 350-

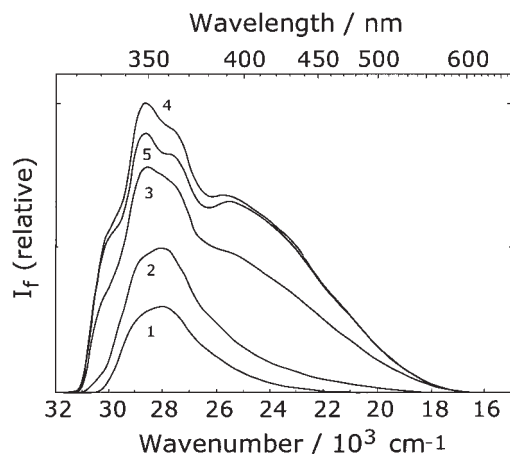


Fig. 4. Fluorescence spectra of MNO ( $5.1 \times 10^{-5}$  mol  $\text{dm}^{-3}$ ) in various buffers. pH: (1) 1.16, (2) 2.78, (3) 3.38, (4) 6.04, and (5) 8.93.  $\lambda_{\text{ex}} = 280$  nm.

nm band fluorescence. As a pH value of the MNO solution is raised, the 350-nm band fluorescence is enhanced in intensity and appears structured. Above about pH 3, the broad, longer-wavelength fluorescence is observed along with the 350-nm band fluorescence. The protonation to the nitrogen atom of MNO hinders the generation of the excited state responsible for the longer-wavelength fluorescence. Consequently, the longer-wavelength fluorescence is most likely related with the flow of the unshared electrons of the nitrogen atom to the naphthalene ring in the excited state. This implies that the longer-wavelength fluorescence is due to the intramolecular charge transfer (ICT) state of MNO. Solvent water molecules around an excited MNO molecule would reorient to stabilize the excited state of MNO. This may be responsible for the large Stokes shift of the longer-wavelength fluorescence.

In the case of 2-naphthalenecarboxylic acid in pH 2.0 buffer, its fluorescence has been found to be remarkably red-shifted relative to that in ethanol, 1,4-dioxane, and acetonitrile.<sup>13</sup> The fluorescence of 2-naphthalenecarboxylic acid in water has been assigned to the ICT fluorescence.

**Fluorescence Behavior of MNO in Aqueous Solutions Containing  $\alpha$ -CD.** When  $\alpha$ -CD was added to MNO solution, the absorption peaks of MNO were slightly shifted to longer wavelengths, accompanied by isosbestic points at 299, 323, and 326 nm (not shown). This finding indicates the formation of an inclusion complex of  $\alpha$ -CD with MNO. Figure 5 depicts fluorescence spectra of MNO ( $2.0 \times 10^{-5}$  mol  $\text{dm}^{-3}$ ) in pH 6.1 buffers containing various concentrations of  $\alpha$ -CD. As the  $\alpha$ -CD concentration is increased, the intensity of the 350-nm band fluorescence is enhanced, with a sharpening of the vibrational bands. At the same time, the longer-wavelength fluorescence is reduced in intensity, indicating that the generation of the excited state responsible for the longer-wavelength fluorescence is suppressed by the addition of  $\alpha$ -CD. Because of the hydrophobic environment inside the  $\alpha$ -CD cavity as well as the desolvation of water molecules from an MNO molecule, the longer-wavelength fluorescence is weakened by the formation of the  $\alpha$ -CD-MNO inclusion complex, compared to the 350-nm band fluorescence. This is consistent with our assignment that the longer-wavelength fluorescence is the ICT emission. When

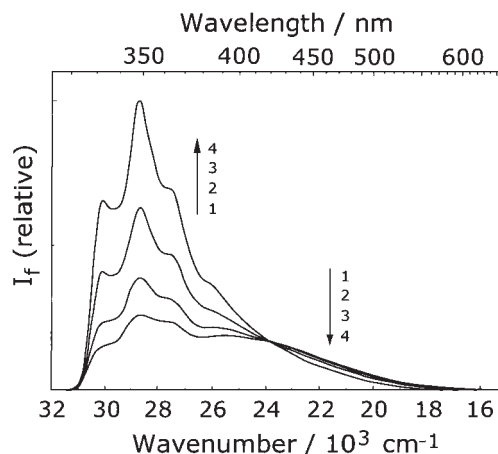
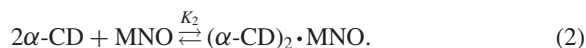


Fig. 5. Fluorescence spectra of MNO ( $2.0 \times 10^{-5}$  mol  $\text{dm}^{-3}$ ) in pH 6.1 buffers containing various concentrations of  $\alpha$ -CD. Concentration of  $\alpha$ -CD: (1) 0, (2)  $3.0 \times 10^{-3}$ , (3)  $6.0 \times 10^{-3}$ , and (4)  $1.0 \times 10^{-2}$  mol  $\text{dm}^{-3}$ .  $\lambda_{\text{ex}} = 299$  nm.

the  $\alpha$ -CD-MNO inclusion complex has a 1:1 stoichiometry, the Benesi-Hildebrand equation holds:<sup>14,15</sup>

$$1/(I_f - I_f^0) = 1/a + 1/(aK_1[\alpha\text{-CD}]_0). \quad (1)$$

Here,  $I_f$  and  $I_f^0$  are the fluorescence intensities in the presence and absence of  $\alpha$ -CD, respectively,  $a$  is an experimental constant including the fluorescence quantum yields of MNO and the 1:1  $\alpha$ -CD-MNO inclusion complex,  $K_1$  is the equilibrium constant for the formation of the 1:1  $\alpha$ -CD-MNO inclusion complex, and  $[\alpha\text{-CD}]_0$  is the initial concentration of  $\alpha$ -CD. As shown in Fig. 6a, a plot for the 350-nm band fluorescence, which is based on Eq. 1, exhibits a concave curve. A value of the correlation coefficient ( $R^2$ ) is estimated to be 0.9829 for the straight line in Fig. 6a. In addition, a negative  $K_1$  value, which has no physical meaning, is estimated from the straight line drawn in Fig. 6a. These results are inconsistent with the assumption that the stoichiometry of the  $\alpha$ -CD-MNO inclusion complex is 1:1. For 2-methylnaphthalene, 2-chloronaphthalene, naphthol, and 6-bromo-2-naphthol, the formation of 2:1  $\alpha$ -CD-guest inclusion complexes has been reported.<sup>16-21</sup> Thus, we analyzed the inclusion process of the  $\alpha$ -CD-MNO inclusion complex as a 2:1 stoichiometry.



Here,  $K_2$  is the equilibrium constant for the formation of the 2:1  $\alpha$ -CD-MNO inclusion complex ( $(\alpha\text{-CD})_2 \cdot \text{MNO}$ ) from  $\alpha$ -CD and MNO. In this case, the following equation is derived:

$$1/(I_f - I_f^0) = 1/b + 1/(bK_2[\alpha\text{-CD}]_0^2), \quad (3)$$

where  $b$  is an experimental constant including the fluorescence quantum yields of MNO and the 2:1  $\alpha$ -CD-MNO inclusion complex. Figure 6b shows a plot of  $1/(I_f - I_f^0)$  against  $1/[\alpha\text{-CD}]_0^2$ . This plot exhibits a straight line ( $R^2 = 0.9962$ ), indicating that the  $\alpha$ -CD-MNO inclusion complex has a 2:1 stoichiometry. A value (0.9962) of the correlation coefficient in the plot for the 2:1  $\alpha$ -CD-MNO inclusion complex is greater than that (0.9829) for the 1:1  $\alpha$ -CD-MNO inclusion complex, supporting the 2:1 stoichiometry. In the 2:1  $\alpha$ -CD-MNO inclusion complex, an MNO molecule located within the two  $\alpha$ -CD cav-

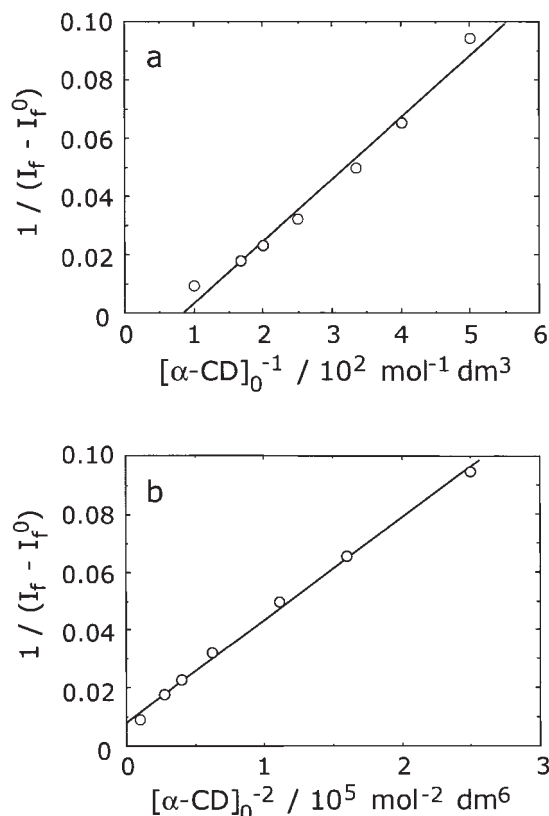


Fig. 6. (a) Plot of  $1/(I_f - I_f^0)$  against  $1/[\alpha\text{-CD}]_0$  for the fluorescence intensities of MNO ( $2.0 \times 10^{-5} \text{ mol dm}^{-3}$ ) in pH 6.1 buffers containing various concentrations of  $\alpha$ -CD.  $\lambda_{\text{ex}} = 299 \text{ nm}$ .  $\lambda_{\text{obs}} = 350 \text{ nm}$ . (b) Plot of  $1/(I_f - I_f^0)$  against  $1/[\alpha\text{-CD}]_0^2$  for the fluorescence intensities of MNO ( $2.0 \times 10^{-5} \text{ mol dm}^{-3}$ ) in pH 6.1 buffers containing various concentrations of  $\alpha$ -CD.  $\lambda_{\text{ex}} = 299 \text{ nm}$ .  $\lambda_{\text{obs}} = 350 \text{ nm}$ .

ities experiences the strongly hydrophobic environment, probably because the two  $\alpha$ -CD molecules are axially bound to an MNO molecule from both its ends. Consequently, the experimental result that the fluorescence spectra of MNO in  $\alpha$ -CD solution are significantly sharpened can be reasonably explained in terms of the formation of the 2:1  $\alpha$ -CD–MNO inclusion complex. From the plot shown in Fig. 6b, a  $K_2$  value of  $34000 \pm 3000 \text{ mol}^{-2} \text{ dm}^6$  is obtained. This  $K_2$  value is about twice the  $K_2$  value ( $16800 \text{ mol}^{-2} \text{ dm}^6$ ) for 2-methylnaphthalene and about half the  $K_2$  value ( $71800 \text{ mol}^{-2} \text{ dm}^6$ ) for 2-chloronaphthalene.<sup>16,17</sup>

**Fluorescence Behavior of MNO in Aqueous Solutions Containing  $\beta$ -CD and  $\gamma$ -CD.** Figure 7 illustrates absorption spectra of MNO ( $5.1 \times 10^{-5} \text{ mol dm}^{-3}$ ) in pH 6.1 buffers containing various concentrations of  $\beta$ -CD. When  $\beta$ -CD is added, the absorption band is shifted to longer wavelengths, accompanied by an isosbestic point at 300 nm. The maximal absorption peak is slightly decreased in intensity. These findings indicate the formation of an inclusion complex between  $\beta$ -CD and MNO. Figure 8 shows fluorescence spectra of MNO ( $2.0 \times 10^{-5} \text{ mol dm}^{-3}$ ) in pH 6.1 buffers containing various concentrations of  $\beta$ -CD. Upon the addition of  $\beta$ -CD, the fluorescence intensity is enhanced, indicating the formation of the  $\beta$ -CD–MNO inclusion complex. The intensity ratio of the longer-

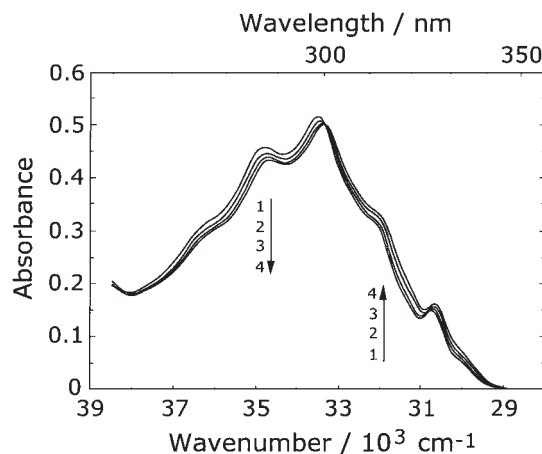


Fig. 7. Absorption spectra of MNO ( $5.1 \times 10^{-5} \text{ mol dm}^{-3}$ ) in pH 6.1 buffers containing various concentrations of  $\beta$ -CD. Concentration of  $\beta$ -CD: (1) 0, (2)  $3.0 \times 10^{-4}$ , (3)  $1.0 \times 10^{-3}$ , and (4)  $3.0 \times 10^{-3} \text{ mol dm}^{-3}$ .

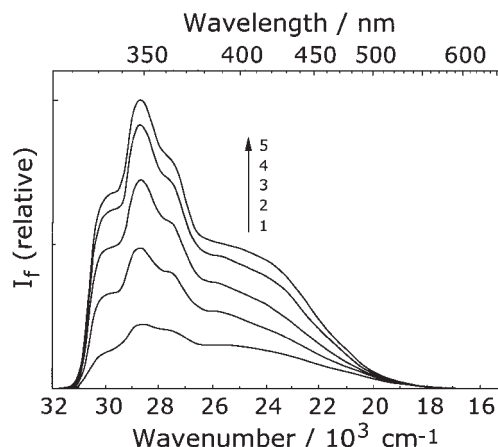


Fig. 8. Fluorescence spectra of MNO ( $2.0 \times 10^{-5} \text{ mol dm}^{-3}$ ) in pH 6.1 buffers containing various concentrations of  $\beta$ -CD. Concentration of  $\beta$ -CD: (1) 0, (2)  $3.0 \times 10^{-4}$ , (3)  $1.0 \times 10^{-3}$ , (4)  $3.0 \times 10^{-3}$ , and (5)  $1.0 \times 10^{-2} \text{ mol dm}^{-3}$ .  $\lambda_{\text{ex}} = 300 \text{ nm}$ .

wavelength fluorescence to the 350-nm band fluorescence is decreased by the addition of  $\beta$ -CD, although the effect of  $\beta$ -CD is not as prominent as the effect of  $\alpha$ -CD (see Fig. 5). The result that the binding of an MNO molecule to the  $\beta$ -CD cavity reduces the intensity of the longer-wavelength fluorescence is due most likely to the hydrophobic environment of the inside of the  $\beta$ -CD cavity as well as to the desolvation of water molecules around an MNO molecule. As in the case of  $\alpha$ -CD, the effects of  $\beta$ -CD on the fluorescence behavior of MNO suggests that the longer-wavelength emission is the ICT fluorescence. The fluorescence spectra in the presence of  $\beta$ -CD are not too sharp compared to those in the presence of  $\alpha$ -CD. With respect to the fluorescence intensity ratio and the sharpening of the fluorescence bands, the smaller effects of  $\beta$ -CD than those of  $\alpha$ -CD indicate that an MNO molecule bound to the  $\beta$ -CD cavity is located in the less hydrophobic environment than an MNO molecule bound to the two  $\alpha$ -CD cavities. This implies that the  $\beta$ -CD–MNO inclusion complex has a 1:1 stoichiometry.



From a plot based on Eq. 1, a  $K_1$  value for  $\beta$ -CD has been evaluated to be  $640 \pm 20 \text{ mol}^{-1} \text{ dm}^3$ . The good fit of the observed data to the straight line confirms the formation of the 1:1  $\beta$ -CD-MNO inclusion complex. The  $K_1$  value for MNO is close to the  $K_1$  value ( $685 \text{ mol}^{-1} \text{ dm}^3$ ) for naphthalene, suggesting that the naphthalene moiety of MNO is incorporated into the  $\beta$ -CD cavity.<sup>15</sup>

Upon the addition of  $\gamma$ -CD, an isosbestic point at 313 nm was observed with a very slight decrease in the absorbance of the maximal peak, which was similarly observed for  $\beta$ -CD (Fig. 7). In the presence of  $\gamma$ -CD, the MNO fluorescence was slightly enhanced, indicating the formation of the  $\gamma$ -CD-MNO inclusion complex. The longer-wavelength fluorescence was very slightly reduced in intensity relative to the 350-nm band fluorescence. From the intensity change in the 350-nm band fluorescence, a  $K_1$  value for the formation of the 1:1  $\gamma$ -CD-MNO inclusion complex was estimated to be  $15 \pm 5 \text{ mol}^{-1} \text{ dm}^3$ . The small  $K_1$  value for  $\gamma$ -CD is reasonable because  $\gamma$ -CD has the largest cavity size among  $\alpha$ -,  $\beta$ -, and  $\gamma$ -CDs. There was no evidence for the formation of a 1:2  $\gamma$ -CD-MNO inclusion complex.

**Fluorescence Behavior of MNO in Aqueous Solutions Containing  $\beta$ -CD and 1-Propanol.** Addition of 1-propanol (PrOH) to MNO solution containing  $\beta$ -CD results in the increase of the 350-nm band fluorescence and the decrease of the longer-wavelength fluorescence (Fig. 9). This finding suggests that a ternary inclusion complex is formed among  $\beta$ -CD, MNO, and PrOH.



Here,  $K_3$  is the equilibrium constant for the formation of the 1:1:1  $\beta$ -CD-MNO-PrOH inclusion complex from the 1:1  $\beta$ -CD-MNO inclusion complex and PrOH. The fluorescence intensity of MNO in aqueous solution containing  $\beta$ -CD and PrOH is represented by

$$I_f = (c + dK_1[\beta\text{-CD}] + eK_1K_3[\beta\text{-CD}][\text{PrOH}]_0)[\text{MNO}], \quad (5)$$

where  $c$ ,  $d$ , and  $e$  are experimental constants including the fluorescence quantum yields of free MNO, the  $\beta$ -CD-MNO inclu-

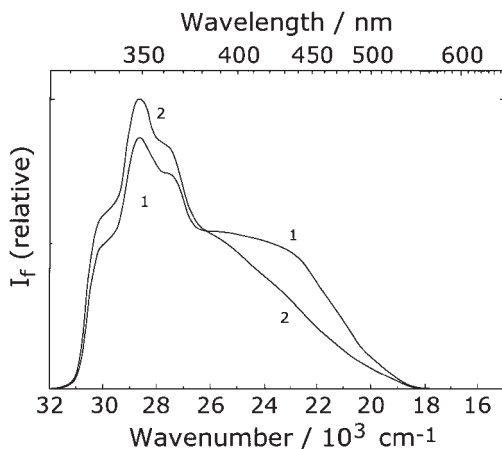


Fig. 9. Fluorescence spectra of MNO ( $2.0 \times 10^{-5} \text{ mol dm}^{-3}$ ) in  $\beta$ -CD solutions (pH 6.1) with (spectrum 2) and without 1-propanol ( $0.4 \text{ mol dm}^{-3}$ ) (spectrum 1).  $\lambda_{\text{ex}} = 300 \text{ nm}$ .

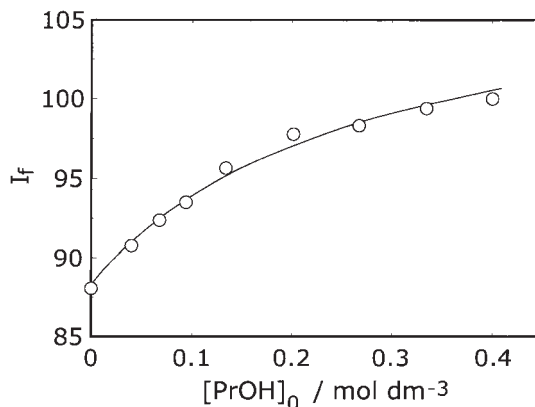


Fig. 10. Simulation of the observed fluorescence intensity data for the formation of the 1:1:1  $\beta$ -CD-MNO-1-propanol inclusion complex. The best fit simulation curve for the 1:1:1 inclusion complex has been calculated under the assumptions of  $c = 1.11 \times 10^5$ ,  $d = 2.06 \times 10^6$ ,  $e = 2.06 \times 10^6 \text{ mol}^{-1} \text{ dm}^3$ , and  $K_3 = 12.1 \text{ mol}^{-1} \text{ dm}^3$ .  $[\text{MNO}]_0 = 2.0 \times 10^{-5} \text{ mol dm}^{-3}$ .  $[\beta\text{-CD}]_0 = 1.0 \times 10^{-2} \text{ mol dm}^{-3}$ .  $\lambda_{\text{ex}} = 300 \text{ nm}$ .  $\lambda_{\text{obs}} = 350 \text{ nm}$ .

sion complex, and the  $\beta$ -CD-MNO-PrOH inclusion complex, respectively, and  $[\text{PrOH}]_0$  is the initial concentration of PrOH. Using the initial concentrations ( $[\beta\text{-CD}]_0$  and  $[\text{MNO}]_0$ ) of  $\beta$ -CD and MNO, the concentrations of free  $\beta$ -CD and free MNO are given as follows:

$$[\beta\text{-CD}] = [\beta\text{-CD}]_0 / (1 + K_4[\text{PrOH}]_0), \quad (6)$$

$$[\text{MNO}] = [\text{MNO}]_0 / (1 + K_1[\beta\text{-CD}] + K_1K_3[\beta\text{-CD}][\text{PrOH}]_0), \quad (7)$$

where  $K_4$  is the equilibrium constant for the formation of the 1:1  $\beta$ -CD-PrOH inclusion complex. A  $K_4$  value has been reported to be  $3.72 \text{ mol}^{-1} \text{ dm}^3$ .<sup>22</sup> Figure 10 shows the best fit simulation curve together with the observed fluorescence intensities as a function of  $[\text{PrOH}]_0$ . From this simulation, a  $K_3$  value of  $12.1 \text{ mol}^{-1} \text{ dm}^3$  is estimated. Values of  $c$ ,  $d$ , and  $e$  are also estimated to be  $1.11 \times 10^5$ ,  $2.06 \times 10^6$ , and  $2.11 \times 10^6 \text{ mol}^{-1} \text{ dm}^3$ , respectively. Because the fluorescence intensity change was small in the  $\beta$ -CD-MNO-1-butanol system, a  $K_3$  value for 1-butanol could not be estimated. This finding suggests that it is difficult for 1-butanol, which is bulkier than PrOH, to form a ternary inclusion complex with  $\beta$ -CD and MNO.

## Conclusion

MNO exhibits dual emissions (the 350-nm band fluorescence (LE emission) and the longer-wavelength emission) in water (pH 6.1 buffer), although it exhibits only a single emission in organic solvents (cyclohexane, ethanol, and acetonitrile). In acidic aqueous solution, MNO shows the 350-nm band fluorescence alone. This suggests that unshared electrons on the nitrogen atom of MNO play a critical role in the appearance of the longer-wavelength fluorescence. Consequently, the ICT state of MNO is most likely responsible for the longer-wavelength fluorescence.  $\alpha$ -CD and  $\beta$ -CD form the 2:1 and 1:1 host-guest inclusion complexes with MNO in pH 6.1 buffers, respectively. The intensity ratio of the longer-wavelength fluorescence to the 350-nm band fluorescence is reduced in CD solution, partic-

ularly in  $\alpha$ -CD solution. This implies that the desolvation of water molecules around an MNO molecule as well as the relatively hydrophobic CD cavity bound to an MNO molecule decelerates the generation of the ICT state responsible for the longer-wavelength fluorescence.

## References

- 1 W. Saenger, *Angew. Chem., Int. Ed. Engl.*, **19**, 344 (1980).
- 2 S. Hamai and A. Nakamura, "Handbook of Photochemistry and Photobiology," ed by H. S. Nalwa, American Scientific Publishers, Stevenson Ranch (2003), Vol. 3, "Supramolecular Photochemistry," Chap. 2.
- 3 R. Chenevert and N. Voyer, *Tetrahedron Lett.*, **25**, 5007 (1984).
- 4 R. Chenevert and R. Plante, *Can. J. Chem.*, **61**, 1092 (1983).
- 5 A. V. Veglia and R. H. de Rossi, *J. Org. Chem.*, **58**, 4941 (1993).
- 6 V. Ramamurthy, *Tetrahedron*, **42**, 5753 (1986).
- 7 M. S. Syamala, B. N. Rao, and V. Ramamurthy, *Tetrahedron*, **44**, 7234 (1988).
- 8 G. S. Cox, P. J. Hauptman, and N. J. Turro, *Photochem. Photobiol.*, **39**, 597 (1984).
- 9 A. Nag and K. Bhattacharyya, *Chem. Phys. Lett.*, **151**, 474 (1988).
- 10 A. Nag and K. Bhattacharyya, *J. Chem. Soc., Faraday Trans.*, **86**, 53 (1990).
- 11 J. Dey, E. L. Roberts, and I. M. Warner, *J. Phys. Chem. A*, **102**, 301 (1998).
- 12 D. LeGourrierec, V. A. Kharlanov, R. G. Brown, and W. Rettig, *J. Photochem. Photobiol., A*, **130**, 101 (2000).
- 13 S. Hamai, *Chem. Phys. Lett.*, **267**, 515 (1997).
- 14 H. A. Benesi and J. H. Hildebrand, *J. Am. Chem. Soc.*, **71**, 2703 (1949).
- 15 S. Hamai, *Bull. Chem. Soc. Jpn.*, **55**, 2721 (1982).
- 16 S. Hamai, *J. Inclusion Phenom. Mol. Recognit. Chem.*, **27**, 57 (1997).
- 17 S. Hamai, *J. Phys. Chem. B*, **101**, 1707 (1997).
- 18 S. Hamai and K. Hori, *Supramol. Chem.*, **10**, 43 (1999).
- 19 H. Park, B. Mayer, P. Wolschann, and G. Köhler, *J. Phys. Chem.*, **98**, 6158 (1994).
- 20 S. Hamai, *J. Chem. Soc., Chem. Commun.*, **1994**, 2243.
- 21 S. Hamai, *J. Phys. Chem.*, **99**, 12109 (1995).
- 22 Y. Matsui and K. Mochida, *Bull. Chem. Soc. Jpn.*, **52**, 2808 (1979).